# Diagnosing temperature change inside sonoluminescing bubbles by calculating line spectra

Yu An[1,2] and Chaohui Li[1]
[1]*Department of Physics, Tsinghua University, Beijing 100084, China*
[2]*Institute of Acoustics, Chinese Academy of Science, Beijing 100190, China*
(Received 4 April 2009; published 28 October 2009)

With the numerical calculation of the spectrum of single bubble sonoluminescence, we find that when the maximum temperature inside a dimly luminescing bubble is relatively low, the spectral lines are prominent. As the maximum temperature of the bubble increases, the line spectrum from the bright bubble weakens or even fades away relative to the background continuum. The calculations in this paper effectively interpret the observed phenomena, indicating that the calculated results, which are closely related to the spectrum profile, such as temperature and pressure, should be reliable. The present calculation tends to negate the existence of a hot plasma core inside a sonoluminescing bubble.

DOI: 10.1103/PhysRevE.80.046320 PACS number(s): 78.60.Mq, 32.70.Jz, 33.70.Jg

Cavitation is known to lead to an extreme condition of high pressure and high temperature inside the cavitation bubble [1–4]. However, due to the small dimensions (micron size) of the bubble and the short duration (hundreds of picoseconds) of the extreme condition, this temperature is difficult to measure. Thus, sonofusion experiments [5–7] have caused controversy [8,9] rather than a sensation: except for counting very few emitted neutrons, there is no other way to determine whether the temperature inside the bubble could meet the criteria for thermonuclear fusion. A few years ago, moving single bubble sonoluminescence (SBSL) in 85% sulfuric acid ($H_2SO_4$) was observed. The bubble was thousands of times brighter than the SBSL in water ($H_2O$) [10]. In addition, the prominence of atomic and ionic spectral lines or bands could be measured [11]. Therefore, it was assumed that a high temperature plasma core existed inside the sonoluminescing bubble. Nevertheless, no other evidence was found to support this supposition.

Recently, experiments have detected stable SBSL in 85% $H_2SO_4$ with similar brightness [12,13]. Although the brightness of the sonoluminescing bubble may be roughly indicative of the temperature, we have found that some SBSL bubbles of a larger size are much brighter than the hotter, but smaller, ones. In fact, the brightness is correlated with both the maximum temperature and the bubble size [14]. Some of the SBSL spectra look similar to a blackbody radiation spectrum [15,16], and it is possible to obtain the fitted temperature using the blackbody radiation formula. However, it is unreasonable to simply take the fitted temperature as the real temperature inside the sonoluminescing bubble for a number of reasons. First of all, the temperature inside the bubble varies temporally and spatially as the bubble flashes. Second, many of the sonoluminescing bubbles are not opaque [17], a condition inappropriate for the application of the blackbody radiation formula. Lastly, the wavelength range of the SBSL spectrum (200–800 nm) is too narrow to obtain a reliable fitted temperature [18].

Since a direct measurement of the temperature inside the bubble is impossible, one may suggest an indirect way, for instance through calculations. A numerical simulation can prove quite helpful in this type of situation. In general, the calculation involves partial differential equations of the fluid mechanics and depends on many thermodynamic parameters of the gases and the liquids, as determined by experiments [18]. In addition, the slightly different Rayleigh-Plesset (RP) equations [19] governing the bubble motion result in a relatively large difference to gas dynamics [20]. The question then arises with respect to the reliability of these types of calculated results. The latest SBSL calculation illustrates that the emission of an atomic or molecular line spectrum competes with the processes of the free-free or free-bound continuum, and the relative strength between these is sensitively dependent on temperature [17]. When the temperature inside the bubble is around 10 000 K, the emission of an atomic or molecular line spectrum dominates the SBSL. As the temperature rises, the emission of the free-free or free-bound continuum gradually overwhelms the spectral line emission processes and the spectral lines gradually merge into the background of the continuum spectrum. Thus, if the calculations can reproduce the phenomena such as the relative strength between the spectral lines and the continuum of the SBSL spectrum, then the other results tightly related to those phenomena, such as the temperature inside the bubble, are likely to be correct.

The present calculation is based on the numerical simulation model reported in Refs. [17,18] but covers the additional computation of molecular, atomic, and ionic spectral lines, as well as their broadening caused by the collisions between particles (atoms, molecules, ions, and electrons) or resonance. In this model, the equations of fluid mechanics of two gas components, i.e., inert gas [21] and water vapor, are employed to describe gas dynamics inside the bubble. The mass action law [22] is applied to evaluate the production of the chemical reaction and the ionization. At the boundary of the bubble, the phase transition of vapor and heat exchange are considered, while outside the bubble, the energy balance equation is solved to calculate the heat flow. The free-free or free-bound continuum processes of the electron-neutral atom bremsstrahlung [23], the electron-ion bremsstrahlung and recombination radiation [24], and the radiative attachment of electrons to atoms and molecules [18,25–27] are included in the light emission calculation. The calculation formulas are almost the same as those deduced in Refs. [17,18], with a few others listed below. First of all, for the RP equation governing the variation of the bubble radius, we adopt the following form:

 

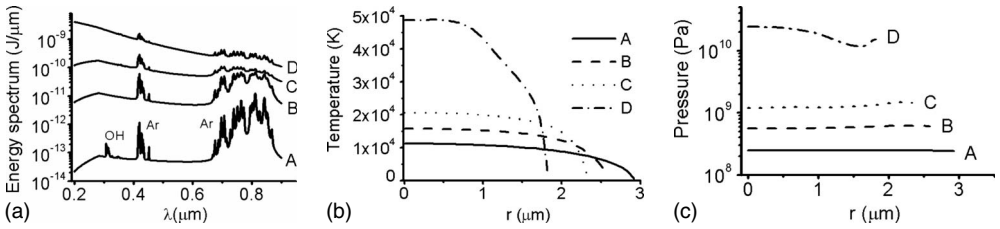


FIG. 1. An Ar bubble in 85% $H_2SO_4$ at 20 °C under four different $p_a$=1.5, 1.7, 2.0, and 4.0 atm marked as A, B, C, and D, respectively. (a) Energy spectra, (b) temperatures as the bubbles are at their minimum size, and (c) corresponding pressures.

$$R\ddot{R} + \frac{3}{2}\dot{R}^2 = \frac{1}{\rho_l}[p_l - p_\infty - p_s(t+t_R)] + \frac{t_R}{\rho_l}\dot{p}_l, \tag{1}$$

where $t$ is the time, $R(t)$ is the radius of the bubble, $p_\infty$ is the ambient pressure, $p_s(t)=-p_a \sin(\omega t)$ is the driving acoustic pressure, $t_R \equiv R/c_l$, $c_l$ is the speed of sound in the liquid at ambient temperature and 1 atm pressure, and $p_l=p_g(R,t) - 4\eta\dot{R}/R - 2\sigma/R$ is the pressure on the liquid side of the bubble wall, $p_g(R,t)$ is the pressure on the gas side of the bubble wall, $\eta$ is the dynamic viscosity, and $\sigma$ is the surface tension coefficient of the liquid. For water, $\rho_l$ and $c_l$ are calculated with the Tait equation, while for 85% $H_2SO_4$, owing to the lack of relevant parameters, $\rho_l$ and $c_l$ are treated as constants. Applying a fixed $\rho_l$ and $c_l$ in Eq. (1) would affect the calculation results; however, since the viscosity and density of 85% $H_2SO_4$ are about 13 and 1.8 times of water, respectively, we find that, unlike the case for water, whether $\rho_l$ and $c_l$ are variable or not, the calculated results do not change substantially. In particular, no significant differences occur in terms of the calculated profile of the spectrum. Second, we suppose that the spectral line emission of Ar or $Ar^+$ is attributed to thermal excitation, and for the transition $i \rightarrow j$, the power of radiation per unit volume may be evaluated as

$$P_{i,j} = \frac{n_a g_i e^{-h\nu_{i,j}/kT}}{\sum_k g_k e^{-E_k/kT}} A_{i,j} h\nu_{i,j}, \tag{2}$$

where $n_a$ is the number density of Ar or $Ar^+$ inside the bubble, $g_i$ is the Landé factor of the $i$th energy level $E_i$, $A_{i,j}$ is the transition probability [28], and $h\nu_{i,j}$ is the photon energy. Finally, for the $O_2$/Ar bubble, the emission of oxygen molecules can be negligible [29]; however, the vibrational and rotational transitions of $A\ ^2\Pi_u \rightarrow X\ ^2\Pi_g$ second negative system of the $O_2^+$ should be taken into account because these spectral lines have been observed in the SBSL spectrum. Using an analogy of the OH radical light emission [25,30–32], we assume that the ionic $O_2^+$ emission is attributed to the chemical excitation, which is supposed to be

$$O + O + M = O_2^+ * + e^- + M. \tag{3}$$

Here, $M$ represents other atoms, molecules, or ions. Considering a transition from the excited state $O_2^+ *$ ($A\ ^2\Pi_u$) with vibrational and rotational quantum numbers $v$ and $J$, respectively, to the $O_2^+$ ($X\ ^2\Pi_g$) state with $v'$ and $J'$, the power of radiation per unit volume of that transition can be calculated as

$$P_{vJ,v'J'} = k_r n_O n_O n_M f \frac{(2J+1)e^{-E(v,J)/kT}}{Q_{v,J}} A_{vib}^{vv'} A_{rot}^{JJ'} h\nu_{vJ,v'J'}, \tag{4}$$

where $n_i$ is the particle number density of $i$ species, $f$ is the factor for estimating the radiation quenching by collisions with other particles [25,33], $Q_{vJ}$ is the partition function, and $E(v,J)$ is the energy of the vibrational and the rotational state $(v,J)$. The relative vibrational transition probability $A_{vib}^{vv'}$ can be found in Ref. [34], and the rotational part $A_{rot}^{JJ'}$ can be evaluated by the *Hönl-London formulas* [31]. The photon energy is given by $h\nu_{vJ,v'J'}$. We notice here that $k_r$ is the coefficient of the reaction rate, but no data are available for the reaction [Eq. (3)]. As a rudimentary attempt, $k_r$ for the reaction $O+H+M \rightarrow OH^*+M$ is applied to the reaction [Eq. (3)]. More details regarding reaction [Eq. (3)] will follow later.

We shall now calculate the case of an argon bubble with an ambient radius $R_0$=13.5 $\mu$m in 85% $H_2SO_4$ at 20 °C at the sound wave frequency $f$=37.8 kHz. The calculated SBSL spectra for four cases are illustrated in Fig. 1(a). The OH radical spectral lines at the region of 0.30–0.36 $\mu$m and Ar atom spectral lines at the regions of 0.41–0.45 $\mu$m and 0.68–0.88 $\mu$m are visible for the case of lowest amplitude of driving acoustic pressure $p_a$=1.5 atm. As $p_a$ increases, the light intensity of the SBSL rapidly goes up and the OH molecular spectral lines quickly disappear as the vapor pressure of 85% $H_2SO_4$ is low. As well, the Ar atom spectral lines gradually diminish relative to the continuum. If one compares these curves to those in Fig. 2a in Ref. [10], the calculated results can be seen to demonstrate a similar trend to that of the measured data in terms of the change of the intensity of the atomic spectral lines relative to the continuum. Some data, such as the ambient radius of bubbles, are not mentioned in Ref. [10], making an exact comparison between the calculation and observation impossible in the present calculation. Nonetheless, the calculated spectrum of the SBSL seems reasonable. Corresponding to the four cases in Fig. 1(a), the distributions of temperature and pressure inside the bubbles, when they are at their minimum size, are illustrated in Figs. 1(b) and 1(c), respectively. When the temperature is below 20 000 K, it is readily apparent that those molecular or atomic spectral lines are prominent at the background of the continuum and that they decline as the temperature rises. These findings reveal that the sonoluminescing bubbles experiencing different maximum temperatures also present different profiles of their spectra. The spectrum

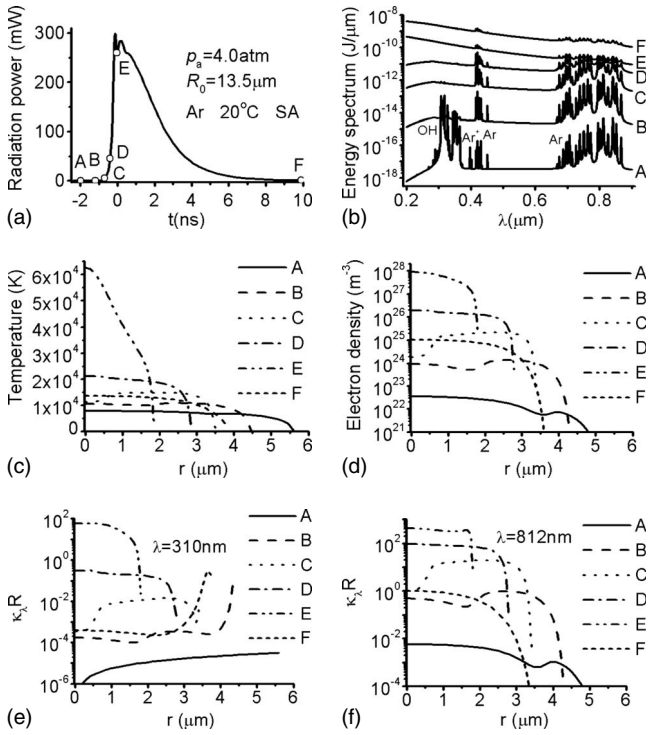


FIG. 2. An Ar bubble in 85% $H_2SO_4$ for case D in Fig. 1. (a) Radiation power of the bubble vs time for moments marked from A to F, (b) energy spectra, (c) temperatures, (d) number densities of ionized electrons, (e) absorption coefficient $\kappa_\lambda$ times the bubble radius $R$ at $\lambda=310$ nm, and (f) at $\lambda=812$ nm.

of the SBSL in $H_2SO_4$ with the prominence of spectral lines probably indicates that the temperature inside the bubble at its minimum size is lower than 20 000 K. However, if only the fuzzy spectral lines appear in the spectrum or the spectrum is just the continuum, the maximum temperature inside the bubble should be higher than or much higher than 20 000 K. In addition, one may notice that there is a huge difference between these temperatures in Fig. 1(b) and the blackbody fit temperatures in Fig. 2b in Ref. [10].

Recently, the streak camera has captured the way in which the spectral continuum gradually overwhelms the atomic spectral lines within a single flash duration of a bright SBSL [13]. Since some parameters, such as the ambient radius of the bubble, are not provided in the paper, we will not process the exact simulation of the measured data. However, we are able to reproduce this observed phenomenon with the numerical simulation and can even diagnose the temperature changes inside the sonoluminescing bubble during one flash period. We choose the case of $p_a$=4.0 atm in Fig. 1. Figure 2(a) illustrates the radiation pulse per flash of this bubble, and we select six moments during the flash, i.e., points A–F, to evaluate the time-dependent radiation energy spectrum [see Fig. 2(b)] and corresponding temperatures and number densities of the electron [see Figs. 2(c) and 2(d)]. Since the radiation energy spectrum is a time-accumulating effect of light emission, it always increases as time progresses. As the radiation power increases from A to E [see Fig. 2(a)], the entire background of the continuum rises. The OH lines in the region of 0.30–0.36 $\mu$m and the $Ar^+$ ionic lines near 0.4 $\mu$m quickly disappear, while the prominence of the Ar atom spectral lines at the regions of 0.41–0.45 $\mu$m and 0.68–0.88 $\mu$m gradually decreases [see Fig. 2(b)]. At F, the light goes out and the corresponding energy spectrum divided by the sound wave period is just the radiation power observed in experiments.

From A to E, there is an obvious increase in temperature and electron number density [see Figs. 2(c) and 2(d)]. The ionized electron number increases with the temperature, but the ionization consumes a substantial amount of thermal energy and hinders the further increase of that temperature. Through calculation, we find that if no molecular dissociation and ionization were to take place, the maximum temperature inside this bubble would be 220 000 K instead of 60 000 K. In addition, at the center of the bubble, almost all of the atoms are ionized, but as the temperature decreases along the bubble radius, the number density of ionized electron rapidly declines [see the curves in Fig. 2(d)]. This indicates that the ionization is sensitive to the temperature. In the present calculation, only the ionization of one electron from one atom is considered. If the temperature gets much higher, the ionization of the second electron of the atom should also be taken into account and there should be a greater consumption of the thermal energy. The ionization energy of the second electron is much higher, and its ionization should prevent any further increase in the temperature. Thus, it seems to be impossible to reach a temperature of millions of degrees inside the bubble, through acoustic cavitation, because all of the electrons in the atom should be taken off in order to reach that temperature.

On the other hand, the intensity of the spectral lines relative to the continuum is of significant concern in terms of the absorption coefficient $\kappa_\lambda$. For the transparent case $\kappa_\lambda R \ll 1$, the spectral lines may appear, while for the opaque case $\kappa_\lambda R \gg 1$, these lines are suppressed. For $\lambda=310$ nm, the bubble remains transparent most of the time, only becoming opaque at its maximum temperature [see Fig. 2(e)]. The absence of the OH lines at 310 nm is due to too few OH radicals and their radiations are overwhelmed by the continuum. For $\lambda=812$ nm, in cases D and E, except for the inner rim, the bubble is opaque [see Fig. 2(f)], which means that during the flash, it is mostly opaque [see Fig. 2(a)]. However, the Ar atomic lines at vicinity of 812 nm are visible even though they look fuzzy at the end. There are two reasons for this. (1) The spectra of Fig. 2(b) are accumulated results; for example, at moment C, the bubble is not completely opaque [see Fig. 2(f)]. Therefore, the line spectrum emission occurs, which will scrape up to the spectrum; (2) at moment D, the inner rim of the bubble is still transparent where the line spectra survive.

Relatively speaking, explaining the appearance of an $O_2^+$ ionic line spectrum in the SBSL is problematic. Since the excitation energy of $O_2^+$ is about 18 eV, which corresponds to a temperature of 180 000 K or so, it is natural and understandable that one assumes the occurrence of a hot plasma core inside the bubble when the temperature of a blackbody fit is only about 10 000 K [10]. However, in the present calculation, the maximum temperature inside the sonoluminescing bubble is a few tens of thousands of degrees. Plasma forms in the center of the bubble but it is not hot enough

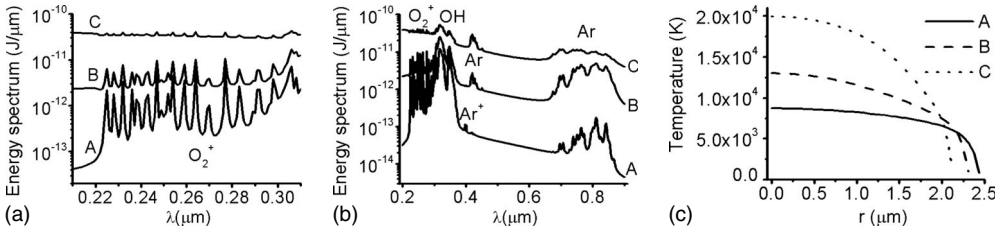


FIG. 3. A bubble filled with 50% Ar and 50% $O_2$ in 85% $H_2SO_4$ at 20 °C under three different $p_a$=1.9, 2.2, and 2.5 atm marked as A, B, and C, respectively. (a) Energy spectra of $O_2^+$ ions at the range of 0.21–0.31 $\mu$m, (b) energy spectra at the range of 0.2–0.9 $\mu$m, and (c) the maximum temperatures.

either to produce the high-energy electron that may excite $O_2^+$ via impact or to thermally excite a sufficient amount of $O_2^+$. The only possible choice in the present model is to assume that the $O_2^+$ is excited through a chemical reaction. However, we find that the reaction rate of the possible reaction $O+O^+=O_2^++h\nu$ is too low [35] to effectively interpret the observation. The other possible two body reactions, such as $O_2+e=O_2^+*+2e$, are less important because most of the oxygen molecules in a high temperature circumstance are already decomposed into the atoms. In addition, the high pressure and high temperature circumstance inside the bubble is usually favorable for a three body reaction. Therefore, we have to assume that the $O_2^+$ is excited through a three body reaction. Analogizing to the excitation process of the OH radical [25,30–32] with which we have successfully interpreted the OH radical spectral lines in SBSL [17], we further assume that the three body chemical reaction is what is expressed in Eq. (3). Our trial calculation excludes another possible process: $O+O^++M=O_2^+*+M$. As mentioned earlier, there are no data for $k_r$ for the reaction [Eq. (3)], and in addition, some parameters are not provided in the experimental reports [10,11]. Therefore, the following calculation remains tentative: since the $O_2^+$ ionic spectral lines are observed in 85% $H_2SO_4$ gassed with a mixture of $O_2$ and inert gas, as a trial calculation, the bubble is assumed to be filled with a 50% Ar and 50% $O_2$ mixture, and its light emission processes are computed. For the bubble with ambient radius of 13.5 $\mu$m in 85% $H_2SO_4$ at 20 °C, we compare three cases with different $p_a$. The spectrum of $A\ ^2\Pi_u \rightarrow X\ ^2\Pi_g$ second negative system of $O_2^+$ is at the range of 0.21–0.31 $\mu$m, as shown in Fig. 3(a). These $O_2^+$ ionic spectral lines are obvious for the $p_a$=1.9 atm case and gradually weaken as $p_a$ increases. For $p_a$=2.5 atm, the spectrum almost merges into the continuum background. Compared to the emission intensity in Fig. 1, prominent $O_2^+$ ionic spectral lines appear in the spectrum of the dimly luminescing bubble, similarly to the prominent Ar atomic spectral lines, which is qualitatively consistent with the experimental observations [11]. Figure 3(b) shows a wider spectrum range and it more clearly demonstrates that both the $O_2^+$ ionic and Ar atomic spectral lines evolve in a similar manner. It is obvious that the maximum temperature inside the bubble increases with $p_a$ [see Fig. 3(c)], but these temperatures are merely a few tens of thousand degrees. In fact, it is the chemical dissociation of $O_2$ that prevents the increase of the temperature inside the bubble. One may notice that although $p_a$ =2.0 atm for bubble C in Fig. 1, its maximum temperature is about 20 000 K. In contrast, for bubble B in Fig. 3, filled with a 50% Ar and 50% $O_2$ mixture, $p_a$=2.2 atm can only achieve a maximum temperature of about 13 000 K. Figure 4 shows that in the latter case, most of the $O_2$ molecules are decomposed to O atoms, known as the process of decalescence, whereas in the former case, there are only a few water vapor molecules involved in chemical reactions. It is obvious that a higher $O_2$ composition inside the bubble leads to a lower maximum temperature.

In contrast to the SBSL in $H_2SO_4$, where the appearance of an atomic line spectrum of a noble gas is common [10], the typical spectrum of the SBSL in water is usually featureless and a line spectrum is rarely observed [12]. To understand this phenomenon, we consider the case of an argon bubble with the ambient radius of $R_0$=4.0 $\mu$m in water. Figure 5 shows the SBSL spectra and the corresponding maximum temperatures and pressures for three different cases. For the dimmest bubble, the molecular and atomic spectra are prominently visible although the Ar atomic lines near 0.8 $\mu$m are broadened to a band [see curve A in Fig. 5(a)]. As the SBSL intensifies, these molecular and atomic spectra rapidly merge into the continuum background and only small fuzzy ripples remain, which are hard to recognize as molecular or atomic spectral lines [see curves B and C in Fig. 5(a)]. On the other hand, comparing curves B and C in Fig. 5(b) with curve D in Fig. 1(b), we notice that although the maximum temperatures of cases B and C are lower than that of case D in Fig. 1, the spectral lines of case D are clearer. This is because the definition of the spectral line in the SBSL spectrum is dependent not only on the maximum temperature but also on the pressure. Comparing curves B and C in Fig. 5(c) with curve D in Fig. 1(c), we find that the pressure in case D is much lower. Since the viscosity of $H_2O$ is much lower than that of $H_2SO_4$, in general, the bubble compression in water is more severe. In addition, much more vapor remains inside the bubble in $H_2O$ and, as the bubble collapses, the vapor dissociates into monoatoms. The van der Waals

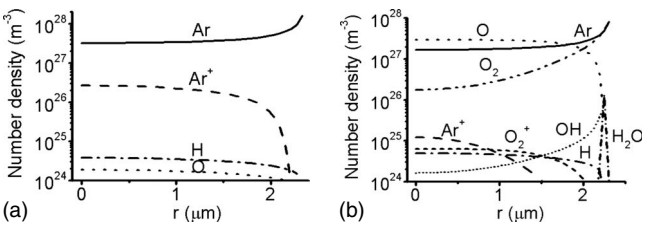


FIG. 4. The particle number densities inside the bubble corresponding to (a) case C in Fig. 1 and (b) case B in Fig. 3.

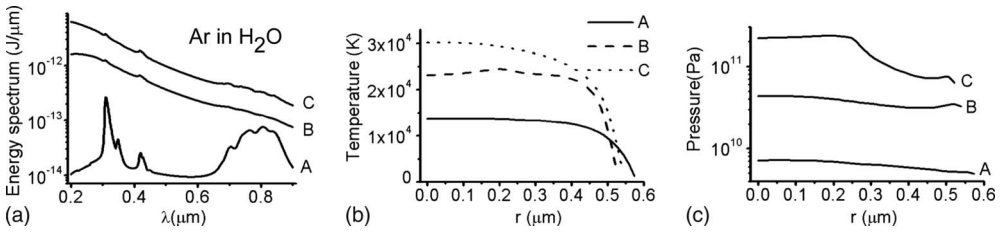


FIG. 5. An Ar bubble with $R_0=4.0$ $\mu$m in water: (A) at 20 °C $H_2O$, $f=33.8$ kHz and $p_a=1.22$ atm; (B) at 20 °C $H_2O$, $f=33.8$ kHz and $p_a=1.32$ atm; and (C) at 0 °C $H_2O$, $f=31.9$ kHz and $p_a=1.32$ atm. (a) Energy spectra, (b) the maximum temperatures, and (c) corresponding pressures.

excluded volume increases, which leads to the increase in pressure and the enhancement of the collision broadening of spectral lines. For this reason, spectral lines of the SBSL were previously observed in $H_2SO_4$ but not in $H_2O$.

The present calculation can effectively interpret the observed phenomena that concern the line spectrum of the SBSL. Therefore, these calculated results of temperature and pressure, which are tightly connected with the spectrum profile, should be reasonable. When the maximum temperature is relatively low, SBSL bubbles of the same size are dim and the spectral lines are prominent. As the maximum temperature increases, the bubble gradually becomes bright and the spectral lines turn weak or even disappear into the continuum background. That is, the spectral line emission dominates the dim SBSL (usually with lower temperature), whereas the continuum dominates the bright SBSL (usually with higher temperature). The reasons are (a) although the emission intensity of both the continuum and the spectral lines increases with temperature, the increase in the continuum is much faster than that of the spectral lines and (b) in general, the temperature and pressure inside the bubble increase together, and the increase in collision broadening of the spectral lines follows. Similar phenomena can take place during a single flash period of the SBSL. On the other hand, we find that although there is an extreme difference in the brightness between the SBSL in $H_2O$ and that in $H_2SO_4$, the maximum temperatures inside the bubbles are of the same order of magnitude, namely, tens of thousands of degrees. It is the ionization that prevents the further enhancement of the maximum temperature inside the bubble. At higher temperatures, more electrons are ionized and more thermal energy is consumed.

Project No. 10974116 supported by NSFC.

[1] H. Frenzel and H. Schultes, Z. Phys. Chem. Abt. B **27**, 421 (1934).
[2] D. F. Gaitan, L. A. Crum, C. C. Church, and R. Roy, J. Acoust. Soc. Am. **91**, 3166 (1992).
[3] B. P. Barber and S. J. Putterman, Nature (London) **352**, 318 (1991).
[4] M. P. Brenner, S. Hilgenfeldt, and D. Lohse, Rev. Mod. Phys. **74**, 425 (2002).
[5] R. P. Taleyarkhan *et al.*, Science **295**, 1868 (2002).
[6] R. P. Taleyarkhan *et al.*, Phys. Rev. E **69**, 036109 (2004).
[7] R. P. Taleyarkhan *et al.*, Phys. Rev. Lett. **96**, 034301 (2006).
[8] D. Shapira and M. Saltmarsh, Phys. Rev. Lett. **89**, 104302 (2002).
[9] C. G. Camara, S. D. Hopkins, K. S. Suslick, and S. J. Putterman, Phys. Rev. Lett. **98**, 064301 (2007).
[10] D. J. Flannigan and K. S. Suslick, Nature (London) **434**, 52 (2005).
[11] D. J. Flannigan and K. S. Suslick, Phys. Rev. Lett. **95**, 044301 (2005).
[12] Junfeng Xu *et al.*, Phys. Rev. E **76**, 026308 (2007).
[13] Weizhong Chen *et al.*, Phys. Rev. E **78**, 035301(R) (2008).
[14] An Yu, Chin. Phys. B **17**, 2984 (2008).
[15] R. Hiller, S. J. Putterman, and B. P. Barber, Phys. Rev. Lett. **69**, 1182 (1992).
[16] P. T. Greenland, Contemp. Phys. **40**, 11 (1999).
[17] Y. An and C. Li, Phys. Rev. E **78**, 046313 (2008).
[18] Yu. An, Phys. Rev. E **74**, 026304 (2006).
[19] L. Rayleigh, Philos. Mag. **34**, 94 (1917); M. Plesset, ASME Trans. J. Appl. Mech. **16**, 277 (1949); B. Noltingk and E. Neppiras, Proc. Phys. Soc. London, Sect. B **63**, 674 (1950); J. B. Keller and I. I. Kolodner, J. Appl. Phys. **27**, 1152 (1956).
[20] Y. An and C. F. Ying, Phys. Rev. E **71**, 036308 (2005).
[21] D. Lohse, M. P. Brenner, T. F. Dupont, S. Hilgenfeldt, and B. Johnston, Phys. Rev. Lett. **78**, 1359 (1997).
[22] L. D. Landau and E. M. Lifshitz, *Statistical Physics*, 2nd ed. (Pergamon Press, New York, 1980).
[23] S. Geltman, J. Quant. Spectrosc. Radiat. Transf. **13**, 601 (1973).
[24] S. Hilgenfeldt, S. Grossmann, and D. Lohse, Nature (London) **398**, 402 (1999).
[25] K. Yasui, Phys. Rev. E **64**, 016310 (2001).
[26] D. Hammer and L. Frommhold, Phys. Rev. E **65**, 046309 (2002).
[27] L. M. Branscomb, in *Atomic and Molecular Processes*, edited by D. R. Bates, (Academic Press, New York, 1962), pp. 100–138.
[28] Yu. Ralchenko, A. E. Kramida, J. Reader, and NIST ASD Team, NIST Atomic Spectra Database, Version 3.1.5, 2008, http://physics.nist.gov/asd3
[29] P. H. Krupenie, J. Phys. Chem. Ref. Data **1**, 423 (1972).
[30] L. S. Bernstein *et al.*, J. Phys. Chem. **100**, 6612 (1996).
[31] G. Herzberg, *Molecular Spectra and Molecular Structure*,

Spectra of Diatomic Molecules Vol. 1 (Van Nostrand Reinhold, New York, 1950).
[32] R. Mavrodineanu and H. Boiteux, *Flame Spectroscopy* (Wiley, New York, 1965), p. 341.
[33] T. Carrington, J. Chem. Phys. **30**, 1087 (1959).
[34] D. Robinson and R. W. Nicholls, Proc. Phys. Soc. **71**, 957 (1958).
[35] J. Woodall, M. Ag'undez, A. J. Markwick-Kemper, and T. J. Millar, The UMIST Database for Astrochemistry, 2006, http://www.udfa.net/